

## Analysis of DevR regulated genes in *Mycobacterium tuberculosis*

Arnab Bandyopadhyay · Soumi Biswas  
· Alok Kumar Maity · Suman K Banik\*

Received: date / Accepted: date

**Abstract** The DevRS two component system of *Mycobacterium tuberculosis* is responsible for its dormancy in host and becomes operative under hypoxic condition. It is experimentally known that phosphorylated DevR controls the expression of several downstream genes in a complex manner. In the present work we propose a theoretical model to show role of binding sites in DevR mediated gene expression. Individual and collective role of binding sites in regulating DevR mediated gene expression has been shown via modeling. Objective of the present work is two fold. First, to describe qualitatively the temporal dynamics of wild type genes and their known mutants. Based on these results we propose that DevR controlled gene expression follows a specific pattern which is efficient in describing other DevR mediated gene expression. Second, to analyze behavior of the system from information theoretical point of view. Using the tools of information theory we have calculated molecular efficiency of the system and have shown that it is close to the maximum limit of isothermal efficiency.

**Keywords** *Mycobacterium tuberculosis* · Dormancy · Two component system · Information theory

### 1 Introduction

*Mycobacterium tuberculosis* is one of the most well studied human pathogen that causes around 2 million deaths each year. Persistency of *M. tuberculosis* in human body, sometimes for decades, makes it most deadly compared to other human pathogens. While residing within the human body *M. tuberculosis* experiences different kind of stresses and/or signals in the form of chemical components. Most of these signals are sensed by the well defined two component systems (TCS). In

---

Arnab Bandyopadhyay · Soumi Biswas · Suman K Banik (E-mail: skbanik@jcbose.ac.in)

Department of Chemistry, Bose Institute, 93/1 A P C Road, Kolkata 700009, India.

Tel.: +91-33-2303-1142, Fax: +91-33-2303-6790

Alok Kumar Maity

Department of Chemistry, University of Calcutta, 92 A P C Road, Kolkata 700009, India.

\*Corresponding author

order to respond to different environmental stimuli *M. tuberculosis* has developed 11 well defined TCS (Bretl et al 2011) among which DevRS is one of the most studied one and is particularly responsible for dormancy of *M. tuberculosis* in host. Likewise other TCS in bacteria (Appleby et al 1996; Bijlsma and Groisman 2003; Cotter and Jones 2003; Hoch 2000; Laub and Goulian 2007), DevRS is comprised of membrane bound sensor kinase DevS and cytoplasmic response regulator DevR. DevRS TCS becomes active under hypoxic, nitric oxide or nutrient starvation conditions through autophosphorylation of DevS (Betts et al 2002; Voskuil et al 2003; Wayne and Sohaskey 2001). Recent studies reveal that carbon monoxide and ascorbic acid environment can also activate this TCS (Kumar et al 2008; Shiloh et al 2008; Taneja et al 2010). When phosphorylated at the histidine domain DevS transfers its phosphate group to the aspartate domain of DevR. The phosphorylated DevR ( $R_p$ ) acts as transcription factor for  $\sim 48$  genes as well as exerts positive feedback on its own operon. Most of the genes controlled by  $R_p$  contain 20 bp long palindromic sequence (the Dev box) in their upstream region where phosphorylated DevR can bind (Park et al 2003). *Rv3134c* along with *devRS* operon contains two such Dev boxes.  $R_p$  binds to these two boxes and exerts a strong positive feedback as an effect of which *devRS* is cotranscribed along with *Rv3134c* (see Fig. 1).

In the present study a theoretical model has been developed that can qualitatively describe the dynamical behavior of DevR regulated genes. To this end we have chosen four well studied genes *Rv3134c*, *hspX*, *narK2* and *Rv1738* to illustrate DevR controlled regulation and effect of different binding sites in the activation of the four genes (Chauhan and Tyagi 2008a,b; Chauhan et al 2011). The *Rv3134c* and *hspX* promoter sites contain two and three DevR binding sites, respectively. Whereas, *narK2* and *Rv1738* both share the same promoter site containing four binding sites (see Fig. 2). Although these four genes are well studied experimentally further analysis is necessary in connection to the complex interaction between DevR and binding sites. Through modeling we show that how these binding sites control the gene expression individually and collectively. In addition, the proposed model simulates temporal dynamics of different mutants that have been studied experimentally. From this knowledge we predict temporal dynamics of several other mutants which provide qualitative aspects of DevR mediated gene expression. In addition, we propose a general expression pattern for DevR regulated genes which might work well for other DevR controlled gene expression.

We further analyze the proposed model from information theoretical point of view to understand the role of different binding sites. Information theory intrinsically takes care of generalized concept of communication (Shannon 1948). Information processing in biological systems has been successfully analyzed using this concept (Schneider and Stephens 1990; Schneider 1991a,b, 1994, 1997a, 1999, 2000; Hengen et al 1997; Shultzaberger et al 2007). Using the concept of information theory we have shown that our model parameters are in linear relationship with the individual information of sequences. Another important aspect of information theoretical study is the measurement of isothermal molecular efficiency that has a maximum limit of 70% (Schneider 2010). In the present study, we show that DevR controlled promoter sequences have efficiency around 60-65%, thus following the general trend of isothermal efficiency.

## 2 The model

To understand the dynamics of DevR regulated genes in *M. tuberculosis*, we propose in the following a theoretical model based on mass action kinetics of DevR-promoter interaction. The proposed model describes qualitative features of the wild type strain as well as the behavior of some novel mutants. Objectives of the proposed model are following. First, the developed model has been utilized to describe temporal dynamics of DevR regulatory genes in terms of fold induction. Second, after being successful in reproducing qualitative features of the wild type strain, we make *in silico* testable predictions for some novel mutants.

### 2.1 Rv3134c-devRS operon

As mentioned earlier a typical TCS consists of a periplasmic sensor domain and a cytoplasmic response regulator and most importantly this composite system needs a stimulus to make the circuit operative. Similar to other TCS, DevRS gets activated under hypoxic condition (Park et al 2003). Here DevS and DevR are the sensor protein and the response regulator protein, respectively. Once the system is active, DevS gets auto-phosphorylated at the histidine residue and forms phosphorylated DevS which then transfers the phosphate group to its cognate partner DevR to generate pool of phosphorylated DevR. Phosphorylated response regulator ( $R_p$ ) binds to two upstream binding sites of its own operon that leads to co-transcription of Rv3134c along with *devRS* (see Fig. 1). Dual binding at the promoter site is necessary, as mutation (single or double) at these binding sites causes loss in gene expression (Chauhan and Tyagi 2008a).

Outcome of the activation of Rv3134c-*devRS* is to generate pool of phosphorylated response regulator ( $R_p$ ) that controls several downstream genes. In the present model, we follow a simple mechanism for generation of  $R_p$



Eq. (1) takes care of generation and removal of the pool of phosphorylated DevR that acts as a transcription factor for the downstream genes. Since in the present study we are interested only in the dynamics of DevR regulated genes, the minimal kinetics for the generation of  $R_p$  is sufficient to study the dynamics of the downstream genes.

### 2.2 DevR regulated genes

Under hypoxic condition DevRS TCS regulates  $\sim 48$  genes which are broadly classified into four classes, according to the number of Dev boxes (DevR binding site) present in the promoter site (Chauhan et al 2011). In the present work we only deal with four genes (Rv3134c, *hspX*, *narK2* and Rv1738) which have been extensively studied experimentally (Chauhan and Tyagi 2008b). The main reason behind choosing these genes is that they are well characterized and experimental data for mutation in the binding sites of these genes are available (Chauhan and Tyagi 2008b). In addition, experimental temporal dynamics of these genes serves as an

excellent basis for validation of our theoretical model. Before proceeding further, we would like to mention that the four selected genes can be categorized into three different classes based on the number of available DevR binding boxes (see Fig. 2). The most simple case is Rv3134c containing only two Dev boxes and belongs to class I. In *hspz*, that belongs to class II, there are three Dev boxes. A complex four DevR binding box structure is present for genes *nark2*-Rv1738 and are grouped into class III.

### 2.2.1 Rv3134c

Rv3134c gene is the simplest in construct compared to other DevR regulated genes. It has two Dev boxes, one is primary and another is secondary. Phosphorylated DevR ( $R_p$ ) binds to both the primary ( $P$ ) and the secondary ( $S$ ) binding sites (Fig. 2). Kinetics for binding of  $R_p$  to these sites can be modeled as

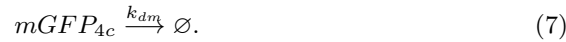


In the above two equations  $P$ ,  $S$  and  $P^*$ ,  $S^*$  stand for inactive and active states of the primary and the secondary binding sites, respectively. Under non-inducing condition both primary and secondary binding sites do not produce any basal level of mRNA whereas the activated sites transcribe in a bulk amount,

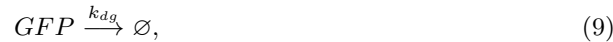
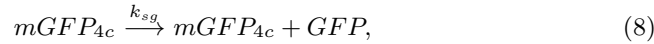


Here  $mGFP_{4c}$  is the mRNA transcribed from Rv3134c. The rate constants  $k_{sm1}$  and  $k_{sm2}$  give a measure of individual contribution from primary and secondary binding sites, respectively, and  $k_{sm3}$  is the measure of co-operative contribution to the transcription of mRNA. The logic behind assuming this kind of equations is the following. When transcription factor binds to any single site (primary or secondary) it is ready to generate transcripts. If both of the sites are occupied by transcription factor then one helps another and a co-operative effect comes into play to produce large amount of transcripts, compared to the transcripts generated from single site occupancy (primary or secondary) as observed in the wild type and single binding box deleted mutants (Chauhan and Tyagi 2008a). Advantage of this approach is that, if only one site is occupied, the cooperative contribution becomes zero automatically, which helps us to generate temporal dynamics of different mutants.

In addition to the above transcription kinetics we consider natural degradation of produced mRNA



The transcribed mRNA then gets translated into protein



where  $GFP$  is the translated protein with a natural degradation given by Eq. (9). It is important to mention that in the experimental setup a promoter-GFP construct has been used to study the promoter activity (Chauhan and Tyagi 2008a,b). This we incorporate in the present model through production of GFP out of the transcripts generated from the promoter. For the rest of the promoters ( $hspX$ ,  $narK2$  and Rv1738), we follow the same strategy to study *in silico* promoter activity.

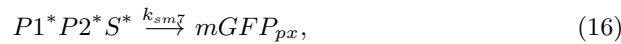
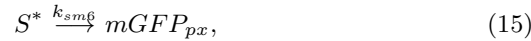
Rv3134c is the operon for DevR regulon and has two binding sites, one is primary and another is secondary. It is not really clear whether the  $S$  binding site which we are considering as *secondary* is actually secondary or not because if one observes  $P$  and  $S$  sites closely there is virtually no difference. From information theoretical analysis (Chauhan et al 2011) it is also evident that both sites have almost the same Ri value (18.2 for  $P$  and 18.3 for  $S$ ), which means almost same amount of energy dissipation occurs during binding. Moreover, according to the sequence walker method (Schneider 1997b) both sites have almost identical contact with protein during binding. This suggest that architecture of this promoter could be  $P$ - $P$  rather than  $P$ - $S$ . Since, both sites are almost identical in structure, one would expect equal contribution from both of them in transcription and hence we assume individual contribution of both binding sites to be equal.

### 2.2.2 $hspX$

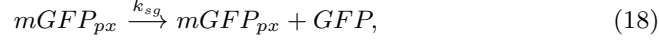
Promoter of  $hspX$  gene contains three binding sites of which two are primary and one is secondary (Chauhan and Tyagi 2008b). Out of the two primary binding sites one is proximal to the transcription start point while the other is distal. While modeling dynamics of these binding sites we have denoted the proximal primary binding site as  $P2$ , the distal primary binding site as  $P1$  and the secondary binding site as  $S$ . When transcription factor binds to these sites they become active,



The activated states  $P1^*$ ,  $P2^*$  and  $S^*$  are ready for making the transcripts. As before, we take individual contribution as well as collective effect during production of transcripts



From the generated transcripts  $mGFP_{px}$  we have considered synthesis of proteins along with its degradation,

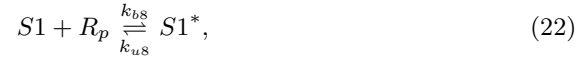


In *hspX* as  $P2$  and  $S$  are nearer to the transcription start point they mostly control expression of this gene, which can be verified by observing the individual contribution of these two sites in the model. As the distance between  $P1$  and  $S$  is large,  $P1$  hardly helps to incorporate co-operative effect and hence plays little role in regulating expression of *hspX* which we will discuss later.

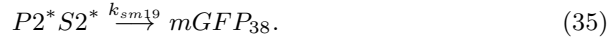
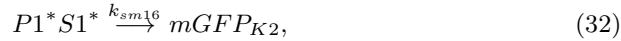
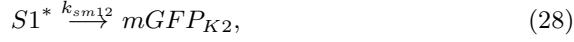
### 2.2.3 *narK2*-Rv1738

This system has four binding sites among which two are primary ( $P1$  and  $P2$ ) and two are secondary ( $S1$  and  $S2$ ).  $P1$  and  $S1$  are nearer to the transcription start site of *narK2* compared to  $P2$  and  $S2$ . Note that the binding sites  $P1$ ,  $S2$  and  $P2$  have been identified earlier and was denoted as  $D1$ ,  $D2$  and  $D3$ , respectively (Chauhan and Tyagi 2008b). The binding site  $S1$  was identified later (Chauhan et al 2011). While developing our model we have followed the recent nomenclature (Chauhan et al 2011). Earlier we have mentioned that the proximal binding sites play a major role in transcription compared to the distal binding sites. So  $P1$  and  $S1$  contribute mostly to the transcription of *narK2* not only because they are located nearer but also for the co-operative effect between them. Similarly, for the Rv1738 promoter,  $P2$  and  $S2$  are nearer to the transcription start site and hence contribute more than  $P1$  and  $S1$  towards making the transcripts. In addition, there is also a cooperative effect between them. As the distance between  $P1$ ,  $S2$  and  $P2$ ,  $S1$  is large, collective cooperative effect can not be operative here. There are always a relative competition between two pairs as they are transcribing in opposite direction and share the same promoter site. Experimental result suggest that expression of Rv1738 remains always high compared to expression of *narK2* (Chauhan and Tyagi 2008b). At this point it is important to mention that in the *narK2*-Rv1738 system transcriptional interference is operative due to overlapping divergent promoter structure (Shearwin et al 2005). However, to keep the model simple we do not consider the mechanism of transcriptional interference in the present work.

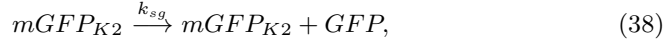
Similar to the previous cases we first generate the activated states of each binding sites as follows,



The activated states are able to generate transcripts for both *narK2* and Rv1738,



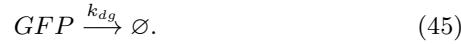
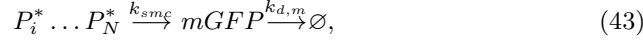
Degradation of mRNA and GFP production have been modeled in a similar fashion,



As mentioned in the work of Chauhan et al (2011), for *narK2* promoter *P1* and *S1* play a major role whereas for Rv1738 promoter *P2* and *S2* play the major role, though all of them are common for both promoters. This in turn affects behavior of their mutants. So, there is a clear division among these four binding sites and moreover, secondary binding sites basically help the primary binding sites through co-operative effect. Hence, while formulating our model we have taken two co-operative contributions. By choosing proper parameter values of the rate constants for the above kinetics, one can describe temporal dynamics of wild type and various mutants in terms of fold induction of GFP, which we have discussed in the next section.

From the above discussion, one can generalise the model and can describe dynamics of any DevR regulated promoter. For a promoter site containing *N*

number of binding sites the kinetics will be,



Where  $k_{smi}$  ( $i \in \{1, N\}$ ) are the individual contribution of the  $N$ -th binding site and  $k_{smc}$  are the measure of co-operative contribution from all the  $n$  binding sites.

### 3 Results and Discussions

To check the validity of our proposed model, developed in the previous section, the kinetic equations (1-40) have been translated into sets of nonlinear ordinary differential equations (ODEs) (see Appendix). To study temporal behavior of the wild type strain and the different mutants, sets of nonlinear ODEs are solved by XPP (<http://www.math.pitt.edu/~bard/xpp/xpp.html>) using the parameter set given in Tables 1-2. The parameter set listed in the tables were guessed to generate the temporal experimental profile given in Figures 3,9,10.

#### 3.1 Wild type

In Fig. 3, we compare numerical results with experimental data for time evolution of relative GFP level for the promoters of *Rv3134c*, *hspX*, *narK2* and *Rv1738*. In the work of Chauhan and Tyagi (2008b) GFP levels have been measured in the unit of RFU/OD. To compare the experimental data with numerical simulation results, we have scaled all the experimental data by the maximum expression level of *Rv1738*, (among the four genes *Rv1738* is the most expressive one; see Fig. 8 of Chauhan and Tyagi (2008b)) so that we get a dimensionless relative expression level for all the four genes. For comparison numerical data has been scaled by using the same strategy. From Fig. 3 it is evident that our model captures the qualitative aspects of the *in vivo* experimental results. In addition, our model could reproduce the competition between *narK2* and *Rv1738* as they share same promoter.

#### 3.2 The mutants

Being successful in describing temporal evolution of the four DevR regulated wild type strains we now look at behavior of their respective mutants. While generating behavior of a specific mutant we have set the value of respective binding and unbinding rate constant to zero.

As mentioned earlier *Rv3134c* promoter has two binding sites, one is primary and other is secondary. However, from their interaction with DevR it is not easy to



detect the difference. Only way to make the distinction is to look at the expression level of different mutants (see Fig. 4). When the primary site is mutated (pmutP) the expression level decreases as expected but on the other hand, expression level is very much similar compared to pmutS where secondary site has been mutated. But for pmutPS, where both sites are mutated, expression level is also same as pmutP or pmutS. This is quite unlikely as both of them should contribute to the generation of transcript. It might happen that, other than *P* and *S* there is a third binding site that contributes to the expression of pmutPS strain. This needs further careful experimental verification. It is important to note that, expression level of the double mutant pmutPS is almost not detectable from our model. According to Chauhan and Tyagi (2008a), expression of pmutP or pmutS decreases  $\sim 25$  fold compared to the wild type expression at 48 hours which is very much close to our simulation result (see Fig. 5).

*hspX* promoter has three binding sites, two are primary and one is secondary (see Fig. 6). Among the two primary sites one is proximal, another is distal. The two primary binding sites were identified by Park et al (2003) and the secondary binding site was identified by Chauhan et al (2011). When the distal primary site *P1* is mutated it can recover GFP expression level  $\sim 70\%$  of wild type expression but if the proximal binding site *P2* is mutated it recovers  $\sim 53\%$  of wild type expression which is also revealed from our model (see Fig. 7). Interestingly, when mutations are done on both primary sites (*P1* and *P2*) our model shows a minimal expression ( $\sim 12\%$  of wild type expression) which is in agreement with the experimental data of Park et al (2003). We have also created double mutants pmutP2S and pmutP1S *in silico* where expression level for pmutP2S1 is undetectable and shows the importance of nearer binding site (*P2* and *S*) on gene expression.

Among the four binding sites in the intergenic sequence of *narK2*-Rv1738 promoter *P1* and *S1* majorly control the transcription of *narK2*. On the other hand, *P2* and *S2* control the transcriton of Rv1738. Effect of Dev box mutation for this promoter has been studied by Chauhan and Tyagi (2008b) by means of GFP reporter assay. At this point it is important to mention that, two sets of mutant data are available in the literature, one is for plate format and the other is for tube format. The main difference between the two format is duration of experiment. The tube format needed twenty days for complete monitoring of the assay and the plate format needed five days. As the tube format takes larger time, there might be food limitations and other factors affecting growth of the colony and hence nonlinear degradation of proteins may play a role during the experiment. As we do not explicitly incorporate nonlinear degradation of proteins in our model, we only consider experimental data obtained from the plate format.

Out of the four binding sites present in the intergenic region of Rv1738-*narK2*, *S1* has been identified recently (Chauhan et al 2011) and the other three sites (*P1*, *P2* and *S2*) were identified earlier by Chauhan and Tyagi (2008b) (see Fig. 2). Secondary binding sites mainly help primary binding sites via co-operatively but their contribution alone towards transcription is low. On the other hand, primary binding sites without any co-operative effect have potential to generate a good amount of transcripts. This is also evident from the mutational analysis of Dev boxes for *narK2*-Rv1738 system.  $G_4$ ,  $G_5$ ,  $G_6$  and  $C_8$  are the most conserved bases for a Dev box which have been selectively deleted to create mutants (Chauhan et al 2011).

For the mutant pAmutP1, where mutation has been done on  $P1$  (a primary binding site for  $narK2$ ) expression level is minimum and is almost not detectable. From this result it can be inferred that contributions from  $P2$  and  $S2$  are really negligible in  $narK2$  expression. In another mutant pBmutP2,  $P2$  is mutated. As  $P2$  mainly controls expression of Rv1738, level of transcript goes down very much and is also not detectable. At the same time, expression of  $narK2$  for this mutant is quite good in comparison to pAmutP1 (see Figs. 9,10). Actually, there is no difference in construct between pAmutP2 and pBmutP2, as in both case  $P2$  site has been mutated (see Fig. 8). For the mutant pBmutP1, expression of Rv1738 is 75% of that of the wild type strain, as  $P1$  site is far upstream of the transcription start point of Rv1738 and has little contribution in transcription. It is clear from the expression of these mutants that there are two co-operative effects operative in  $narK2$ -Rv1738 system, one between  $P1$  and  $S1$  and another between  $P2$  and  $S2$  which we have incorporated in our model. From the close position of the two secondary sites  $S1$  and  $S2$  one might expect a third co-operative contribution, but surprisingly it does not exist as they together cannot recruit  $R_p$  to the primary sites. Similarly, when  $S2$  is mutated (pAmutS2), we observe the same expression level of  $narK2$  as it was for pAmutP2. But expression level decreases for Rv1738 and becomes 25% of that of the wild type strain. When both primary sites are mutated (pAmutP1P2 and pBmutP1P2), as expected, expression level for both genes vanishes almost completely.

Among the  $narK2$  double mutants, pAmutP2S1 and pAmutS1S2 have same expression, which clearly depicts that contribution from  $P2$  and  $S2$  are same but comparatively lower than  $P1$  site, as the expression of pAmutP1S1 and pAmutP1S2 are very small compared to the wild type expression (see Fig. 11). Another interesting point is that expression of pAmutP2S2 is nearly 70% of that of wild type expression but expression of pAmutP2S1S2 is only 35% and pAmutP1P2S2 is almost zero (see Figs. 11,12). Previously we have mentioned that though individual contribution of secondary site is low, co-operative contribution which operates through the secondary site is not negligible. This becomes clear from the nature of these mutants. Except pAmutP2S1S2, other triple mutants have very low expression due to the very obvious reason of  $P1$  deletion. By the similar reasoning, except pBmutP1S1, all other double mutants of Rv1738 have very low expression compared to the wild type strain. This reveals importance of  $P2$  and  $S2$  on gene expression (see Fig. 13). The minute difference in the expression between pBmutS1 and pBmutP1S1 can be explained due to low contribution of  $P1$  in the expression of Rv1738 gene, while it plays a vital role for  $narK2$ . This in fact justifies our model which incorporates two cooperative contribution for the  $narK2$ -Rv1738 system. All the triple mutants of Rv1738 have significantly low expression due to the loss of dual co-operative contribution (see Fig. 14).

From the analysis mentioned above one can conclude that our model is really efficient in describing the temporal dynamics of wild type strain and some mutants. Unfortunately our model could not explain the behavior of single mutants of  $narK2$  gene. If one clearly observes the % expression of  $narK2$  mutants one can see that they are very low ( $\sim 6\%$ ). At such a low expression level, fluctuations in the experimental data play a dominant role, which is difficult to ignore even when the experiments are performed in a bulk culture. Probably, a stochastic version of the present model will be able to remove the anomaly between experimental and theoretical data, which we plan to study in the near future. However, an

important pattern for DevR regulated gene expression that evolves out of this analysis worth mentioning at this point. If a promoter site has a construct with both primary and secondary binding sites with co-operativity in binding between them, then mutation in primary binding site can not be recovered (as revealed from the expression level) by the system. But if the same happens with the secondary binding site then the system recovers itself partly but not as much as it was in the wild type. Though individual contribution of secondary binding site is quite low compared to the primary binding site, co-operative effect that comes through the secondary binding site plays an important role which can not be ruled out. Though apparently, it may look like the primary binding site has major role in transcription, we show that the secondary binding site also play a nontrivial role in the gene expression mechanism through co-operativity.

### 3.3 Parameter sensitivity analysis

To check the sensitivity of the parameter set (listed in Tables 1-2) on the steady state level of mRNA we have used the formalism of total parameter variation developed by Barkai and Leibler (1997). In this formalism, initially all or a subset of rate constants are subjected to random perturbation. In our case, the perturbation is drawn from a random gaussian distribution whose mean is the unperturbed value of each rate constant. In addition, variance of the random gaussian distribution has been considered to be a certain percentage (up to maximum of 10%) of each rate constant. After perturbation, we thus have two sets of parameters. The first set consists of unperturbed (reference) rate constants,  $k_i^0$  and the second set consists of perturbed (modified) rate constants,  $k_i$ . Using these two parameter sets one can compute the level of  $mGFP_{38}$ ,  $mGFP_{K2}$ ,  $mGFP_{px}$  and  $mGFP_{Ac}$  at steady state. The sensitivity in four different reference mRNA levels with respect to model parameters can be characterized by total parameter variation  $\log(\kappa)$ , where  $\log(\kappa) = \sum_{i=1}^N |\log(k_i/k_i^0)|$  (Barkai and Leibler 1997).

The results of total parameter variation are shown in Fig. 15. The resultant data suggests that steady state level of all four mRNAs are sensitive (note the spread of ordinate) to complete parameter set (first column of Fig. 15) of the model which have been modified using the scheme described in the previous paragraph. To understand which subset of the complete parameter set is responsible for such fluctuations we selectively perturb the parameters related to the binding-unbinding kinetics and synthesis-degradation kinetics. When the parameters related to the binding-unbinding kinetics are perturbed we see that the steady state mRNA level are not sensitive to the perturbation (note the collapse of red dots on the dashed blue line in the second column of Fig. 15). However, when the parameter set related to the synthesis-degradation kinetics have been modified we see that the modified parameters can recover the fluctuations (third column of Fig. 15) we have observed when the full parameter set has been perturbed (first column of Fig. 15). This result suggest that parameters related to synthesis-degradation kinetics mostly control the steady state mRNA level in our model.

#### 4 Information theoretical analysis of *devR* regulon

Information theory was founded by Claude E Shannon in late 1940's to analyze the signal transduction in electrical circuits while addressing the problem of efficient communication (Shannon 1948; Cover and Thomas 1991). In his work, Shannon showed how to quantify information exchange between two electrical devices in the form of bits. Although it is a general theory for electrical communication, the basic underlying concept can still be applied to various fields including statistical inference, cryptography, quantum computing, networks, communication in neurobiology and in recent times in molecular biology too (Borst and Theunissen 1999; Rhee et al 2012). For example, let us consider the specific or non-specific binding of a transcription factor to a piece of DNA. It is very much obvious that non-specific binding sites are different from that of specific binding sites. One may argue at this point that what makes the binding sites so different so that the transcription factor recognizes them differently and binds to these sites so specifically and precisely? Another example is the restriction enzyme EcoRI, which cuts the pattern 5'-GAATTC-3' throughout the genome. How EcoRI is able to do this so accurately? These questions can be answered with the help of information theory. The non-specific sites do lack of particular information needed for binding of the transcription factor. Exchange of information occurs during DNA-protein interaction and hence could be well applicable in the present study of DevR mediated transcription of downstream genes.

At this point it is important to connect the mechanism of DNA-protein interaction (DevR-promoter interaction considered in the present model) to the mechanism of a molecular machine. A molecular machine is a macromolecule (single or complex) that performs an operation. By operation one means a particular task or a specific function that has to be done by the macromolecular machine for its survival. For example, when the restriction enzyme EcoRI picks a specific sequence (5'-GAATTC-3') from DNA, it acts as a tiny molecular machine capable of making decision. According to the theory of molecular machine, binding of EcoRI to DNA is restricted (or bounded) by the 'machine capacity' while performing the specific job (Schneider 1991a,b). This machine capacity is closely related to Shannon's 'channel capacity'. As long as a molecular machine does not exceed its machine capacity, it may perform the task as precise as it needs for survival. Following Shannon, the channel capacity can be defined as (Shannon 1948)

$$C = W \log_2 \left( \frac{P}{N} + 1 \right),$$

where the bandwidth  $W$  defines the range of frequencies used in communication and  $P/N$  is the 'signal to noise' ratio. In 1959, in the context of satellite communication, efficiency  $\epsilon$  has been defined from the information theoretical point of view (Pierce and Cutler 1959; Raisbeck 1963)

$$\epsilon = \frac{\ln \left( \frac{P}{N} + 1 \right)}{\frac{P}{N}}.$$

In 1991 Schneider utilized the above ideas in explaining the mechanism of a molecular machine (Schneider 1991a,b). Following Schneider's original notation one can

define the channel capacity of a molecular machine as

$$C_y = d_{space} \log_2 \left( \frac{P_y}{N_y} + 1 \right),$$

where  $d_{space}$  is the number of independent parts of a molecular machine,  $P_y$  is the energy dissipated per operation and  $N_y$  is the thermal noise that interferes with the machine during operation. By dividing  $P_y$  by the machine capacity  $C_y$ , one gets to know the number of joules that must be dissipated to gain one bit of information,

$$\epsilon \equiv \frac{P_y}{C_y} \quad (\text{joules per bit}).$$

The minimum energy dissipation can be calculated from the channel capacity or using the second law of thermodynamics as follows

$$\epsilon_{min} = k_B T \ln(2) \quad (\text{joules per bit}),$$

where  $k_B$  is the Boltzmann's constant (in joules per kelvin) and  $T$  is the absolute temperature (in kelvin). In the limit  $P_y \rightarrow 0$ ,  $\epsilon \rightarrow \epsilon_{min}$ , which yields  $\epsilon \geq \epsilon_{min}$ . Now the efficiency of molecular machine has been defined as the minimum possible energy dissipation divided by actual dissipation, i.e.,

$$\epsilon_t \equiv \frac{\epsilon_{min}}{\epsilon},$$

which is nothing but the isothermal efficiency of a molecular machine (Schneider 1991a). Using the channel capacity theorem proposed by Shannon, Schneider has shown that for a real measurable system, efficiency cannot exceed the theoretical limit  $\epsilon_t$ , mentioned above (Schneider 2010). Although, efficiency for both Carnot engine and molecular machine has been derived using the second law of thermodynamics, the latter is applicable only for isothermal processes. For more information regarding the concept of molecular machine and its application we refer to the pioneering work of Schneider (Schneider 1991a,b, 1994, 2010). However, to make the present work self contained we briefly review some of the notions of information theory developed by Schneider (1991a,b), before going into the application of information theory to our work which we have used in analyzing our model.

#### 4.1 Sequence logo of primary and secondary binding sites

Sequence logo is a graphical method which displays the pattern of nucleotides in a set of aligned sequences and also provides an idea of affinity to binding sites or preferable binding sites for a given sequence (Schneider and Stephens 1990). In this method occurrence of a base in a particular position is denoted by the height of that particular base. To signify the conservation at a particular position one needs to look at the frequency of occurrence of the base at that position. At this point it is important to note that Chauhan et al (2011) have drawn the sequence logo for 25 DevR directed primary and secondary binding sites.

If one observes both sequence logos for primary and for secondary binding sites, it reveals that the logo for primary binding site is more dense than the secondary

binding site and hence contains more information (Schneider and Stephens 1990). From this information one can conclude that if a promoter contains both the primary and the secondary binding site then the primary binding site majorly controls the transcription which is strongly supported by the expression of different mutants. For example, the promoter for Rv1738 gene contains four binding sites, two primary (one proximal and one distal) and two secondary (Chauhan et al 2011). If proximal primary binding site is mutated (pBmutD3 following Chauhan and Tyagi (2008b)) the expression decreases remarkably (1% of that of wild type expression). At the same time if the proximal secondary binding site is mutated (pBmutD2 following Chauhan and Tyagi (2008b)), expression level decreases but 30% of that of wild type expression still persists. Interestingly, when the distal primary binding site is mutated (pBmutD1 following Chauhan and Tyagi (2008b)) the expression level remains almost like the wild type. Here it should be noted that for DevR regulon, the distance between the transcription start point and binding site is very important. For a particular binding site if that distance is large then it has little contribution to the transcription irrespective of its being primary or secondary, which is supported by the expression of the mutant pBmutD1.

What makes the primary sites so different from the secondary sites so that it has control over transcription? The sine wave representing the accessibility of a face of DNA (B-form, 10.6 bases of helical pitch) with the major groove centered at positions 4 and 14.6 (Schneider 1991a,b). Sequence conservation peak (above 1 bit) at positions 4, 5 and 7 and a 10.6 base spacing suggest that DevR makes contact in two consecutive major groove through those positions. Hence, these highly conserved positions play a major role in binding which is clear from the EMSA result (Chauhan et al 2011). At the same time if one analyzes the logo of the secondary binding sites following the same procedure, one finds that there are no such conservation at those positions and hence binding is not so strong that ultimately affects the transcription.

From sequence logo one can also judge the DNA bending ability which is an important but common structural aspect during transcription. The logo of 120 Fis binding sites shows high G and C conservation at  $\pm 7$  (Shultzaberger et al 2007) so direct contact to major groove occurs via these positions. But as these positions are close to each other it is difficult to match the D helics into the major groove properly unless DNA bending occurs. At positions  $\pm 4$ ,  $\pm 3$  and  $\pm 2$  (central region) the logo shows mostly A or T conserved which means either direct minor groove contacts or with bending into the minor groove (Schneider 2001). So it may happens that Fis first contacts the sequence and bending occurs after that. Similarly the logo of DevR primary binding sites contain high conservation at positions  $\pm 3$ ,  $\pm 5$ ,  $\pm 7$  (G and C rich) and the central region  $\pm 1$  is A and T rich. In logo the conservation at position  $\pm 1$  is not so high (just greater than 0.5) compared to that of  $\pm 3$ ,  $\pm 5$  and  $\pm 7$  positions (greater than 1). If one observes the EMSA mutated at central positions (M-9+9) by C and G, the binding affinity vanishes completely (see Fig. 5 of Chauhan et al (2011)), but this should not be the case as conservation at these positions are not so high. So one may conclude here that, similar to the previous case discussed, DevR binds first to the sequences and bending happens after that. But this is a theoretical prediction only, actual scenario is definitely very complex and in a real cellular environment several factors might play their role which are yet to be verified experimentally. The outcome of

the above discussion is very important and one should be aware of these facts while making predictions for the expression level of different mutants.

#### 4.2 $R_{sequence}$ and $R_{frequency}$

Transcription factor may bind to many sequences with different affinities. When it binds to a specific site, it gains some information. This leads to a natural question, what controls the affinity of a transcription factor to a specific binding site? Affinity towards a binding site is directly related to the information content of that particular sequence. The high affinity binding sites have a greater probability of stabilising the transcription initiation complex compared to the low affinity binding sites and thus directly regulates the degree of a particular gene expression.

The information of a binding site can be computed by summing the information of each base positions of a sequence (Schneider et al 1986). This is usually done by creating a weight matrix. The *ri* program of Delila was used to create weight matrix by using 25 primary sequences (see supplementary information of Chauhan et al (2011)). The information thus calculated allows one to compare between the affinity for two particular binding sites and helps to measure the binding energies as well. If one observes the information content of the primary and the secondary binding sites carefully it reveals that the primary binding sites generally have more information content than the secondary one which again justifies the importance of the primary binding sites over the secondary binding sites in connection to the control of particular gene expression.

$R_{frequency}$  depends upon the number of sites and size of the whole genome (Schneider 1991a,b). It is a fixed number which counts the minimum number of bits required by a protein to bind to a specific site. when this minimal criterion is fulfilled, binding takes place on a particular site. The genome of *M. Tuberculosis* is  $4.6 \times 10^6$  bp long. When a protein comes to bind, it can bind in two possible orientations at each base pair. So if a protein wants to bind to 18 sites, it has to choose them from the twice  $4.6 \times 10^6$  possible binding sites. Hence, the minimum number of binary choices needed is  $R_{frequency} = \log_2 (2 \times 4 \times 10^6 / 18) \approx 18.72$  bits per site. If one observes the ratio of  $R_{sequence}/R_{frequency}$  of the sequences of T7 promoters in bacteriophage, it is close to 2. It has been proven experimentally that T7 RNA polymerase only uses half of the conserved pattern. In *incD* the ratio is near 3, so at least three proteins can bind independently. Most of the systems (including ours too) have the ratio near to 1, that means there is just enough pattern at ribosome binding sites ( $R_{sequence}$ ) for them to be found in the genetic material of the cell ( $R_{frequency}$ ).

#### 4.3 Information and Energy

From the aforesaid discussion we have learned that by exchanging information, protein can bind to DNA. So the natural question arises: Is information related to binding energy? Before going into the detailed discussion we explore the relation between energy and information.

From the Second Law of Thermodynamics we know the Clausius inequality as

$$dS \geq \frac{dQ}{T}. \quad (46)$$

Here  $S$  is the total entropy of system,  $T$  is the absolute temperature and  $Q$  is the heat. The protein binding process is an isothermal process and the temperature remains same immediately after binding. Integration of the above equation, keeping  $T$  constant yields

$$\Delta S \geq \frac{q}{T}. \quad (47)$$

Using the concepts of statistical mechanics one can write the Boltzmann-Gibbs entropy of a system as

$$S \equiv -k_B \sum_{i=1}^{\Omega} p_i \ln p_i, \quad (48)$$

where  $k_B$  is the Boltzmann constant,  $\Omega$  is the number of possible microstates of the system,  $p_i$  is the probability of the  $i$ -th microstate out of  $\Omega$  and  $\sum_{i=1}^{\Omega} p_i = 1$  for  $p_i \geq 0$ . Following Shannon (1948) one can write the uncertainty in each of the microstates as,

$$H \equiv - \sum_{i=1}^{\Omega} p_i \log_2 p_i. \quad (49)$$

Combining Eqs. (48-49) one can write using  $\log_2(x) = \ln(x)/\ln(2)$ ,

$$S = k_B \ln(2)H. \quad (50)$$

The decrease in entropy for an operating machine can be written as

$$\Delta S = S_{after} - S_{before}, \quad (51)$$

which leads to the following uncertainty in the machine as

$$\Delta H = H_{after} - H_{before}. \quad (52)$$

Now combining Eqs. (50-52) one can write

$$\Delta S = k_B \ln(2) \Delta H. \quad (53)$$

The information gain  $R$  by a machine takes place due to decrease in uncertainty (Shannon 1948), hence one can write

$$R \equiv -\Delta H, \quad (54)$$

which yields the relation

$$\Delta S = -k_B \ln(2)R. \quad (55)$$

Eq. (55) shows how the decrease in entropy of a molecular machine is directly related to the information that it gains during an operation. Now substituting Eq. (55) in Eq. (47) we get the following inequality

$$k_B T \ln(2) \leq \frac{-q}{R}. \quad (56)$$

Eq. (56) shows how the information is related to heat dissipated ( $-q$ ) during an operation. So if a molecular machine gains 1 bit of information ( $R = 1$ ) then minimum amount of heat dissipated by the machine is

$$\epsilon_{min} = k_B T \ln(2) \quad (\text{joules per bit}). \quad (57)$$



A protein binds to different sites of a DNA according to its affinity towards that site, so protein-DNA dissociation constant,  $K_D$  (ratio of rate of association,  $k_b$  and rate of dissociation,  $k_u$ ), varies with sequence. If one thinks from the molecular aspect it is clear that the rate of protein-DNA binding depends upon the diffusion rate of the protein. As it can bind to specific as well as to non-specific sites one can conclude that apparently the ‘on’ rate is independent of binding sequence. As we have discussed previously that a machine should gain some information during a successful operation. Similarly, if a protein binds to a non-specific site having lack of information then unbinding process is equally probable from that site and hence the non-specific site cannot hold the protein to itself. But exactly opposite phenomena happens when protein binds to a specific site containing the proper information and hence the protein-DNA initiation complex is stabilised and gets ready for transcription. From the aforesaid discussion one can conclude that information of a binding site ( $R_i$ ) is linearly related to the logarithm of ‘off’ rate. But is it really true that information has no relation with the  $k_b$ ? To answer this Shultzaberger et al (2007) have shown that  $k_b$  (or  $K_{on}$  according to Shultzaberger et al (2007)) is not completely independent of information.

Information is related to Gibbs Free energy by a version of Second Law of Thermodynamics (Berg and von Hippel 1987, 1988; Barrick et al 1994)

$$R_i \propto -\Delta G. \quad (58)$$

On the other hand Gibbs free energy is related to the dissociation constant via the relation

$$\Delta G \propto \log K_D; \quad K_D = \frac{k_u}{k_b}. \quad (59)$$

Relating Eqs. (58-59) yields

$$R_i \propto -\log \frac{k_u}{k_b}. \quad (60)$$

So the relation between information and  $k_u$  (or  $K_{off}$  according to Shultzaberger et al (2007)) is negatively proportional which means more the information the sequences have, it is more difficult to destabilise the transcription initiation complex. Thus, according to the information theory, information has linear relationship with both the quantity  $K_D$  and  $k_u$  with negative slope. From our model parameter value we observe that such linear relationship holds good pretty well as discussed above (see Fig. 16). Interestingly the  $k_b$  rate remains almost constant as protein binds frequently to a binding site irrespective of its affinity to that particular site (Das et al 2005; Kim et al 1987; Linnell et al 2004; Schaufler and Kleivit 2003; Shultzaberger et al 2007), which is also evident in our case (see the middle panel of Fig. 16).

#### 4.4 Molecular efficiency

The term ‘efficiency’ was first introduced in classical thermodynamics in the context of a heat engine (Callen 1985; Güémez et al 2002; Jaynes 2003) which operates between two reservoirs at temperature  $T_{hot}$  and  $T_{cold}$ ,

$$\eta = \frac{T_{hot} - T_{cold}}{T_{hot}}. \quad (61)$$

But this equation is not valid in the biological context because to get 70% efficiency  $T_{hot}$  and  $T_{cold}$  need to be 1000k and 300k, respectively, which is lethal for biological systems (Jaynes 1988). Another reason due to which it is not applicable in biological systems is the isothermal nature of most of the biological processes. As a result of which one needs an expression for efficiency for isothermal processes (Schneider 1991b). From information theoretic point of view one can measure the isothermal efficiency when a protein gets bound to a specific site by the relation

$$\epsilon_r = \frac{R_{sequence}}{R_{energy}}, \quad (62)$$

where we have defined  $R_{sequence}$  previously. Here  $R_{energy}$  is logarithm of  $K_{spec}$  where  $K_{spec}$  is the ratio of specific and nonspecific binding at a particular site (Schneider 2010)

$$R_{energy} = \log_2 K_{spec} \quad \text{where} \quad K_{spec} = \frac{k_s}{k_n}. \quad (63)$$

Here  $k_s = 1/K_D$  ( $K_D$  values for different binding sites are listed in Table 1). For the binding site P1 which is in the intergenic region of narK2-Rv1738 the  $K_D$  value is  $0.697 \times 10^{-9}$  M. It is important to mention that the nonspecific binding energy is not known for this system. Considering  $\log_2 k_n = 0$  (as the nonspecific binding energy is not known), we find  $R_{energy} \approx \log_2 k_s = 30.41$  (bits per site). Henceforth  $\epsilon_r = 20/30.41 \simeq 0.66$ , where  $R_{sequence} \approx 20$ . So according to our mathematical model efficiency of this system is 66% and if one calculates the efficiency of other primary binding sites by following the same procedure one will find that all  $\epsilon_r$  values are around 60-65% efficient. This is pretty close to the maximum limit of isothermal efficiency of 70% as reported by Schneider (2010). Note that there are many systems like EcoRI, RepA, etc., which has the efficiency close to this maximum limit.

At this point it is important to mention that for primary binding sites the efficiency is quite good but if one calculates the same for secondary binding sites the efficiency will be quite low as many of them have low  $R_{sequence}$  value. This finding is another justification of why the secondary binding sites have lower contribution to transcription compared to the primary binding sites. Beside this, for Rv3134c, both primary and secondary binding sites have similar molecular efficiency which again raise the question that whether the construct is P-P or P-S?

## 5 Conclusion

The DevRS two component system of *M. tuberculosis* is responsible for its dormancy in host and becomes operative under hypoxic condition. It is experimentally known that phosphorylated DevR controls expression of several downstream genes in a complex manner. To understand the mechanism of DevR mediated downstream gene regulation we have developed a theoretical model based on the elementary kinetics of DevR-promoter interaction. The kinetic model we have developed is efficient in describing behavior of some DevR regulated genes. To this end, we have chosen four DevR controlled genes and have shown that our proposed model can qualitatively generate the gene expression profile of the wild type strain

and some novel mutants that are impaired in DevR binding site. The DevR regulated promoter sites have a definite pattern of construction which contains one stronger binding site (primary sites) and nearly located relatively weaker binding site (secondary site). From construction of the binding sites it seems that primary binding sites majorly control the gene expressions mechanism with a little contribution from the secondary binding sites. Through modeling, we have shown that when both sites (primary as well as secondary) impart a co-operative contribution towards the DevR binding mechanism, effect of the secondary binding site is not negligible. This phenomenon can also be understood from expression profile of some mutants we have predicted in the present study. Keeping this binding pattern in mind we have thus proposed a generalized mechanism which can be applied to understand the temporal profile for any DevR regulated genes. From the information theoretical analysis we have seen that the primary binding sites contain more information than the secondary binding sites which justify the above mentioned mechanism of the preference of DevR towards primary binding sites over secondary binding sites. From information theory it is known that the binding rate constants are in a linear relationship with the individual information of the binding sites (Schneider 2010). The parameter sets we have used for modeling could generate this linear relation predicted by information theory (see Fig. 16). Another important aspect information theory predicts is the molecular efficiency. Using information theory it can be shown that maximum limit of isothermal efficiency is 70% (Schneider 2010). From our model we have calculated the molecular efficiency of the system and have shown that it is close to the maximum limit of isothermal efficiency. Thus in totality, the proposed model could recapture the experimental aspects of DevR mediated gene expression and helps one to understand the phenomenon from information theoretic point of view. We hope that our theoretical model and the subsequent analysis will inspire more experiments in coming days to address other critical issues of DevR regulatory networks that are yet to be explored. Information from this new experimental data will help one to build more detailed model in future.

**Acknowledgements** We express our sincerest gratitude to Jaya S Tyagi and Thomas D Schneider for stimulating discussions and suggestions. AB acknowledges CSIR, Government of India, for a research fellowship (09/015(0375)/2009-EMR-I). SB acknowledges support from Centre of Excellence (CoE) at Bose Institute, Kolkata, supported by DBT, Government of India. AKM acknowledges UGC, Government of India, for a research fellowship (UGC/776/JRF(Sc)). SKB acknowledges support from Bose Institute through Institutional Programme VI - Development of Systems Biology.

## Appendix

DevR:

$$\frac{d[R_p]}{dt} = k_{srp} - k_{drp}[R_p]. \quad (64)$$

*Rv3134c*:

$$\frac{d[P^*]}{dt} = k_{b1}[P][R_p] - k_{u1}[P^*], \quad (65)$$

$$\frac{d[S^*]}{dt} = k_{b2}[S][R_p] - k_{u2}[S^*], \quad (66)$$

$$\begin{aligned} \frac{d[mGFP_{4c}]}{dt} &= k_{sm1}[P^*] + k_{sm2}[S^*] + k_{sm3}[P^*][S^*] \\ &\quad - k_{dm}[mGFP_{4c}], \end{aligned} \quad (67)$$

$$\frac{d[GF P]}{dt} = k_{sg}[mGFP_{4c}] - k_{dg}[GF P]. \quad (68)$$

*hspX*:

$$\frac{d[P1^*]}{dt} = k_{b3}[P1][R_p] - k_{u3}[P1^*], \quad (69)$$

$$\frac{d[P2^*]}{dt} = k_{b4}[P2][R_p] - k_{u4}[P2^*], \quad (70)$$

$$\frac{d[S^*]}{dt} = k_{b5}[S][R_p] - k_{u5}[S^*], \quad (71)$$

$$\begin{aligned} \frac{d[mGFP_{px}]}{dt} &= k_{sm4}[P1^*] + k_{sm5}[P2^*] + k_{sm6}[S^*] \\ &\quad + k_{sm7}[P1^*][P2^*][S^*] - k_{dm}[mGFP_{px}], \end{aligned} \quad (72)$$

$$\frac{d[GF P]}{dt} = k_{sg}[mGFP_{px}] - k_{dg}[GF P]. \quad (73)$$

*narK2-Rv1738*:

$$\frac{d[P1^*]}{dt} = k_{b6}[P1][R_p] - k_{u6}[P1^*], \quad (74)$$

$$\frac{d[P2^*]}{dt} = k_{b7}[P2][R_p] - k_{u7}[P2^*], \quad (75)$$

$$\frac{d[S1^*]}{dt} = k_{b8}[S1][R_p] - k_{u8}[S1^*], \quad (76)$$

$$\frac{d[S2^*]}{dt} = k_{b9}[S2][R_p] - k_{u9}[S2^*], \quad (77)$$

$$\begin{aligned} \frac{d[mGFP_{K2}]}{dt} &= k_{sm8}[P1^*] + k_{sm10}[P2^*] + k_{sm12}[S1^*] \\ &\quad + k_{sm14}[S2^*] + k_{sm16}[P1^*][S1^*] \\ &\quad + k_{sm18}[P2^*][S2^*] - k_{dm}[mGFP_{K2}], \end{aligned} \quad (78)$$

$$\frac{d[GF P]}{dt} = k_{sg}[mGFP_{K2}] - k_{dg}[GF P], \quad (79)$$

$$\begin{aligned} \frac{d[mGFP_{38}]}{dt} &= k_{sm9}[P1^*] + k_{sm11}[P2^*] + k_{sm13}[S1^*] \\ &\quad + k_{sm15}[S2^*] + k_{sm17}[P1^*][S1^*] \\ &\quad + k_{sm19}[P2^*][S2^*] - k_{dm}[mGFP_{38}], \end{aligned} \quad (80)$$

$$\frac{d[GF P]}{dt} = k_{sg}[mGFP_{38}] - k_{dg}[GF P]. \quad (81)$$

## References

Appleby JL, Parkinson JS, Bourret RB (1996) Signal transduction via the multi-step phosphorelay: not necessarily a road less traveled. *Cell* 86:845–848

- Barkai N, Leibler S (1997) Robustness in simple biochemical networks. *Nature* 387(6636):913–917
- Barrick D, Villanueva K, Childs J, Kalil R, Schneider TD, Lawrence CE, Gold L, Stormo GD (1994) Quantitative analysis of ribosome binding sites in *E. coli*. *Nucleic Acids Res* 22:1287–1295
- Berg OG, von Hippel PH (1987) Selection of dna binding sites by regulatory proteins. statistical-mechanical theory and application to operators and promoters. *J Mol Biol* 193:723–750
- Berg OG, von Hippel PH (1988) Selection of dna binding sites by regulatory proteins. *Trends Biochem Sci* 13:207–211
- Betts JC, Lukey PT, Robb LC, McAdam RA, Duncan K (2002) Evaluation of a nutrient starvation model of *Mycobacterium tuberculosis* persistence by gene and protein expression profiling. *Mol Microbiol* 43:717–731
- Bijlsma JJ, Groisman EA (2003) Making informed decisions: regulatory interactions between two-component systems. *Trends Microbiol* 11:359–366
- Borst A, Theunissen FE (1999) Information theory and neural coding. *Nat Neurosci* 2:947–957
- Bretl DJ, Demetriadou C, Zahrt TC (2011) Adaptation to environmental stimuli within the host: two-component signal transduction systems of *Mycobacterium tuberculosis*. *Microbiol Mol Biol Rev* 75:566–582
- Callen HB (1985) Thermodynamics and an Introduction to Thermostatistics. John Wiley & Sons, New York
- Chauhan S, Tyagi JS (2008a) Cooperative binding of phosphorylated Devr to upstream sites is necessary and sufficient for activation of the Rv3134c-devrs operon in *Mycobacterium tuberculosis*: implication in the induction of Devr target genes. *J Bacteriol* 190:4301–4312
- Chauhan S, Tyagi JS (2008b) Interaction of Devr with multiple binding sites synergistically activates divergent transcription of nark2-Rv1738 genes in *Mycobacterium tuberculosis*. *J Bacteriol* 190:5394–5403
- Chauhan S, Sharma D, Singh A, Surolia A, Tyagi JS (2011) Comprehensive insights into mycobacterium tuberculosis Devr (Dosr) regulon activation switch. *Nucleic Acids Res* 39:7400–7414
- Cotter PA, Jones AM (2003) Phosphorelay control of virulence gene expression in bordetella. *Trends Microbiol* 11:367–373
- Cover T, Thomas J (1991) Elements of Information Theory. Wiley-Interscience, New York
- Das N, Valjavec-Gratian M, Basuray AN, Fekete RA, Papp PP, Paulsson J, Chattoraj DK (2005) Multiple homeostatic mechanisms in the control of p1 plasmid replication. *Proc Natl Acad Sci U S A* 102:2856–2861
- Güémez J, Fiolhais C, Fiolhais M (2002) Sadi Carnot on Carnot’s theorem. *Am J Phys* 70:42–47
- Hengen PN, Bartram SL, Stewart LE, Schneider TD (1997) Information analysis of fis binding sites. *Nucleic Acids Res* 25:4994–5002
- Hoch JA (2000) Two-component and phosphorelay signal transduction. *Curr Opin Microbiol* 3:165–170
- Jaynes ET (1988) The evolution of Carnot’s principle. In: Erickson GJ, Smith CR (eds) Maximum-Entropy and Bayesian Methods in Science and Engineering, Kluwer Academic Publishers, Dordrecht, The Netherlands, vol 1, pp 267–281
- Jaynes ET (2003) Note on thermal heating efficiency. *Am J Phys* 71:180–182
- Kim JG, Takeda Y, Matthews BW, Anderson WF (1987) Kinetic studies on Cro repressor-operator DNA interaction. *J Mol Biol* 196:149–158
- Kumar A, Deshane JS, Crossman DK, Bolisetty S, Yan BS, Kramnik I, Agarwal A, Steyn AJ (2008) Heme oxygenase-1-derived carbon monoxide induces the mycobacterium tuberculosis dormancy regulon. *J Biol Chem* 283:18,032–18,039
- Laub MT, Goulian M (2007) Specificity in two-component signal transduction pathways. *Annu Rev Genet* 41:121–145
- Linnell J, Mott R, Field S, Kwiatkowski DP, Ragoussis J, Udalova IA (2004) Quantitative high-throughput analysis of transcription factor binding specificities. *Nucleic Acids Res* 32:e44
- Park HD, Guinn KM, Harrell MI, Liao R, Voskuil MI, Tompa M, Schoolnik GK, Sherman DR (2003) Rv3133c/dosr is a transcription factor that mediates the hypoxic response of *Mycobacterium tuberculosis*. *Mol Microbiol* 48:833–843

- Pierce J, Cutler C (1959) Interplanetary communications. In Ordway, F.I. III(ed.), *Advances in space science*, Vol. 1. Academic Press, Inc, NY, pp. 55-109
- Raisbeck G (1963) *Information Theory: An introduction for Scientists and Engineers*. M.I.T. Press, Cambridge, Massachusetts
- Rhee A, Cheong R, Levchenko A (2012) The application of information theory to biochemical signaling systems. *Phys Biol* 9:045,011–045,011
- Schaufler LE, Klevit RE (2003) Mechanism of DNA binding by the ADR1 zinc finger transcription factor as determined by SPR. *J Mol Biol* 329:931–939
- Schneider TD (1991a) Theory of molecular machines. i. Channel capacity of molecular machines. *J Theor Biol* 148:83–123
- Schneider TD (1991b) Theory of molecular machines. ii. Energy dissipation from molecular machines. *J Theor Biol* 148:125–137
- Schneider TD (1994) Sequence logos, machine/channel capacity, Maxwell’s demon, and molecular computers: a review of the theory of molecular machines. *Nanotechnology* 5:1–18
- Schneider TD (1997a) Information content of individual genetic sequences. *J Theor Biol* 189:427–441
- Schneider TD (1997b) Sequence walkers: A graphical method to display how binding proteins interact with DNA or RNA sequences. *Nucleic Acids Res* 25:4408–4415
- Schneider TD (1999) Measuring molecular information. *J Theor Biol* 201:87–92
- Schneider TD (2000) Evolution of biological information. *Nucleic Acids Res* 28:2794–2799
- Schneider TD (2001) Strong minor groove base conservation in sequence logos implies DNA distortion or base flipping during replication and transcription initiation. *Nucleic Acids Res* 29:4881–4891
- Schneider TD (2010) 70 % efficiency of bistate molecular machines explained by information theory, high dimensional geometry and evolutionary convergence. *Nucleic Acids Res* 38:5995–6006
- Schneider TD, Stephens RM (1990) Sequence logos: A new way to display consensus sequences. *Nucleic Acids Res* 18:6097–6100
- Schneider TD, Stormo GD, Gold L, Ehrenfeucht A (1986) Information content of binding sites on nucleotide sequences. *J Mol Biol* 188:415–431
- Shannon CE (1948) The mathematical theory of communication. *Bell Syst Tech J* 27:379–423
- Shearwin KE, Callen BP, Egan JB (2005) Transcriptional interference – a crash course. *Trends Genet* 21:339–345
- Shiloh MU, Manzanillo P, Cox JS (2008) Mycobacterium tuberculosis senses host-derived carbon monoxide during macrophage infection. *Cell Host Microbe* 3:323–330
- Shultzaberger RK, Roberts LR, Lyakhov IG, Sidorov IA, Stephen AG, Fisher RJ, Schneider TD (2007) Correlation between binding rate constants and individual information of *E. coli* Fis binding sites. *Nucleic Acids Res* 35:5275–5283
- Taneja NK, Dhingra S, Mittal A, Naresh M, Tyagi JS (2010) Mycobacterium tuberculosis transcriptional adaptation, growth arrest and dormancy phenotype development is triggered by vitamin C. *PLoS One* 5:e10,860
- Voskuil MI, Schnappinger D, Visconti KC, Harrell MI, Dolganov GM, Sherman DR, Schoolnik GK (2003) Inhibition of respiration by nitric oxide induces a Mycobacterium tuberculosis dormancy program. *J Exp Med* 198:705–713
- Wayne LG, Sohaskey CD (2001) Nonreplicating persistence of Mycobacterium tuberculosis. *Annu Rev Microbiol* 55:139–163

Promoter	Site	$k_b \times 10^{-7}$ (nM <sup>-1</sup> s <sup>-1</sup> )	$k_u \times 10^{-7}$ (s <sup>-1</sup> )	$K_D$ (nM)
Rv3134c	P	1.70	1.0	0.588
	S	1.70	1.0	0.588
<i>hspX</i>	P1	3.413	1.0	0.293
	P2	1.365	8.33	6.102
	S	1.706	16.67	9.771
<i>narK2</i> -Rv1738	P1	1.194	0.833	0.697
	P2	2.559	1.0	0.391
	S1	1.194	16.6	13.903
	S2	1.70	1.66	0.976

**Table 1** List of binding  $k_{bi}$  ( $i = 1 - 9$ ) and unbinding  $k_{ui}$  ( $i = 1 - 9$ ) constants for the promoters Rv3134c, *hspX* and *narK2*-Rv1738. The corresponding  $K_D$  ( $= k_u/k_b$ ) value for each binding site are also given.

Parameter	Value	Description
$k_{srp}$	$4.07 \times 10^{-3}$ nM s <sup>-1</sup>	Synthesis of $R_p$
$k_{drp}$	$1.66 \times 10^{-5}$ s <sup>-1</sup>	Degradation of $R_p$
$k_{sm1}$	$2.44 \times 10^{-4}$ nM s <sup>-1</sup>	Synthesis of $mGFP_{Ac}$ from $P^*$
$k_{sm2}$	$2.44 \times 10^{-4}$ nM s <sup>-1</sup>	Synthesis of $mGFP_{Ac}$ from $S^*$
$k_{sm3}$	$4.90 \times 10^{-3}$ nM s <sup>-1</sup>	Synthesis of $mGFP_{Ac}$ from $P^*S^*$
$k_{dm}$	$8.33 \times 10^{-4}$ s <sup>-1</sup>	Degradation of $mGFP_{Ac}$
$k_{sm4}$	$4.22 \times 10^{-3}$ nM s <sup>-1</sup>	Synthesis of $mGFP_{px}$ from $P1^*$
$k_{sm5}$	$8.13 \times 10^{-4}$ nM s <sup>-1</sup>	Synthesis of $mGFP_{px}$ from $P2^*$
$k_{sm6}$	$1.29 \times 10^{-4}$ nM s <sup>-1</sup>	Synthesis of $mGFP_{px}$ from $S^*$
$k_{sm7}$	$3.25 \times 10^{-3}$ nM s <sup>-1</sup>	Synthesis of $mGFP_{px}$ from $P1^*P2^*S^*$
$k_{dm}$	$8.33 \times 10^{-4}$ s <sup>-1</sup>	Degradation of $mGFP_{px}$
$k_{sm8}$	$5.20 \times 10^{-4}$ nM s <sup>-1</sup>	Synthesis of $mGFP_{K2}$ from $P1^*$
$k_{sm9}$	$1.62 \times 10^{-4}$ nM s <sup>-1</sup>	Synthesis of $mGFP_{38}$ from $P1^*$
$k_{sm10}$	$1.62 \times 10^{-5}$ nM s <sup>-1</sup>	Synthesis of $mGFP_{K2}$ from $P2^*$
$k_{sm11}$	$1.13 \times 10^{-3}$ nM s <sup>-1</sup>	Synthesis of $mGFP_{38}$ from $P2^*$
$k_{sm12}$	$1.62 \times 10^{-5}$ nM s <sup>-1</sup>	Synthesis of $mGFP_{K2}$ from $S1^*$
$k_{sm13}$	$1.62 \times 10^{-5}$ nM s <sup>-1</sup>	Synthesis of $mGFP_{38}$ from $S1^*$
$k_{sm14}$	$1.62 \times 10^{-5}$ nM s <sup>-1</sup>	Synthesis of $mGFP_{K2}$ from $S2^*$
$k_{sm15}$	$7.00 \times 10^{-4}$ nM s <sup>-1</sup>	Synthesis of $mGFP_{38}$ from $S2^*$
$k_{sm16}$	$4.88 \times 10^{-4}$ nM s <sup>-1</sup>	Synthesis of $mGFP_{K2}$ from $P1^*S1^*$
$k_{sm17}$	$1.62 \times 10^{-3}$ nM s <sup>-1</sup>	Synthesis of $mGFP_{38}$ from $P1^*S1^*$
$k_{sm18}$	$3.25 \times 10^{-4}$ nM s <sup>-1</sup>	Synthesis of $mGFP_{K2}$ from $P2^*S2^*$
$k_{sm19}$	$6.10 \times 10^{-3}$ nM s <sup>-1</sup>	Synthesis of $mGFP_{38}$ from $P2^*S2^*$
$k_{dm}$	$8.33 \times 10^{-4}$ s <sup>-1</sup>	Degradation of $mGFP_{K2}$
$k_{dm}$	$8.33 \times 10^{-4}$ s <sup>-1</sup>	Degradation of $mGFP_{38}$
$k_{sg}$	$6.66 \times 10^{-4}$ nM s <sup>-1</sup>	Synthesis of GFP
$k_{dq}$	$1.67 \times 10^{-5}$ s <sup>-1</sup>	Degradation of GFP

**Table 2** List of kinetic parameters (with values) used in the model. Note that, degradation constant ( $k_{dm}$ ) for all four  $mGFP$ -s ( $mGFP_{Ac}$ ,  $mGFP_{px}$ ,  $mGFP_{K2}$  and  $mGFP_{38}$ ) have been considered to be same.

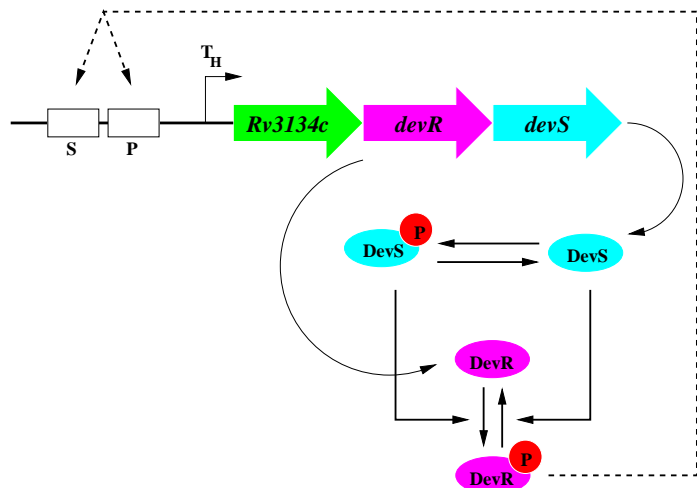


**Fig. 1** Schematic diagram of signal transduction pathway in DevRS two component system. Positive feedback of phosphorylated DevR on its own operon and on *Rv3134c* is shown by the dotted line. Two DevR binding sites S (distal) and P (proximal) are denoted by open boxes.  $T_H$  denotes hypoxia inducible promoter for *Rv3134c*. For simplicity, we do not show mRNA and degradation of proteins in the diagram.

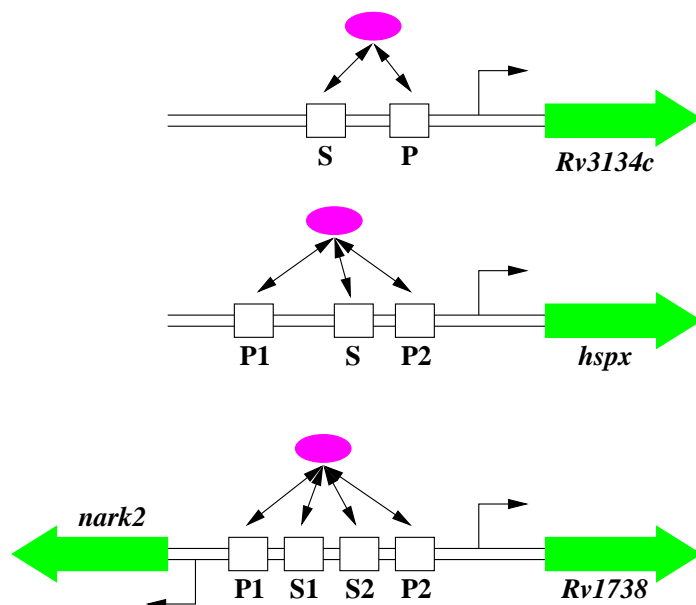


**Fig. 2** Schematic diagram of interaction of phosphorylated DevR with different binding sites (open boxes) of *Rv3134c*, *hspX*, *narK2* and *Rv1738*. *Rv3134c* and *hspX* contains two and three binding sites, respectively. *narK2* and *Rv1738* share same promoter containing four binding sites.



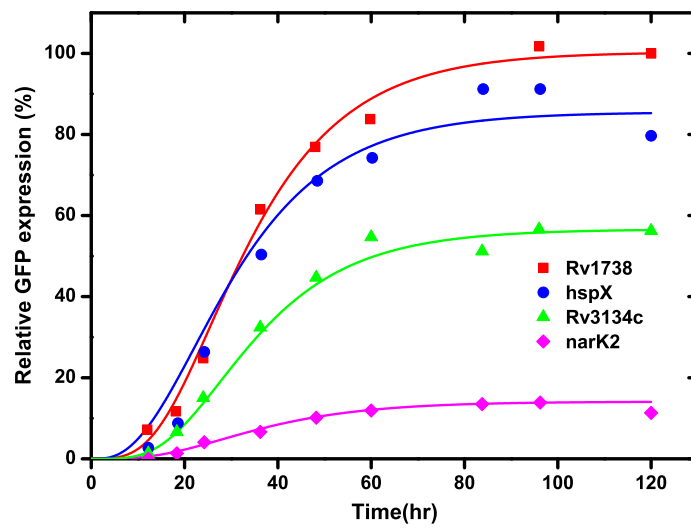


**Fig. 3** Time evolution of relative GFP expression of Rv3134c and three downstream genes. Symbols are taken from Chauhan and Tyagi (2008b) and continuous lines are results of numerical simulation.

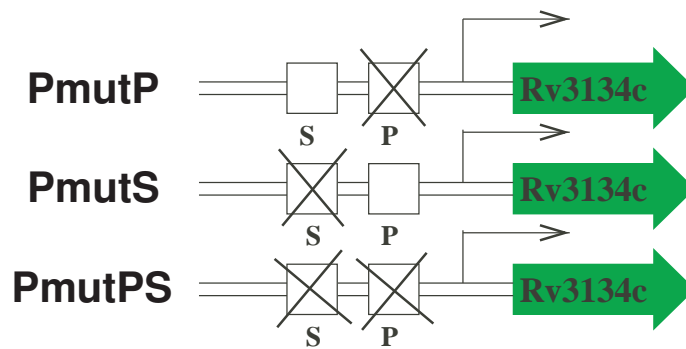


**Fig. 4** Possible mutants by permutation of two binding sites of Rv3134c promoter region. All the three mutants have been studied by Chauhan and Tyagi (2008a).

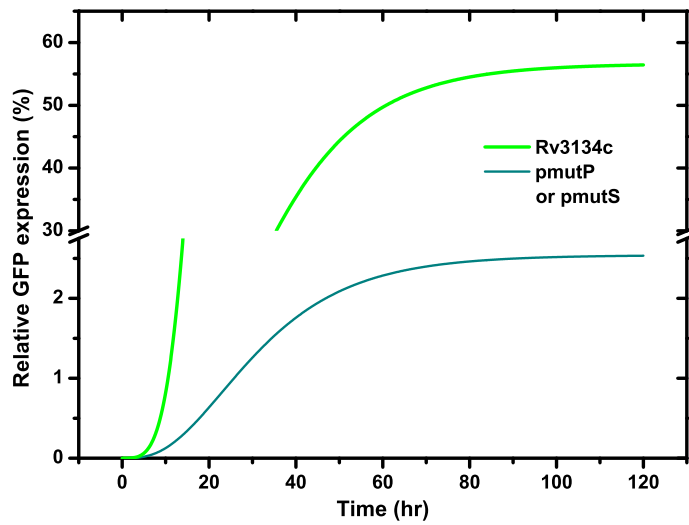


**Fig. 5** Time evolution of Rv3134c (wild type and mutants (pmutP and pmutS)). Expression of mutants is significantly low which is shown by axis breaking. According to our model, expression of the double mutant pmutPS vanishes completely, hence is not shown in the figure.

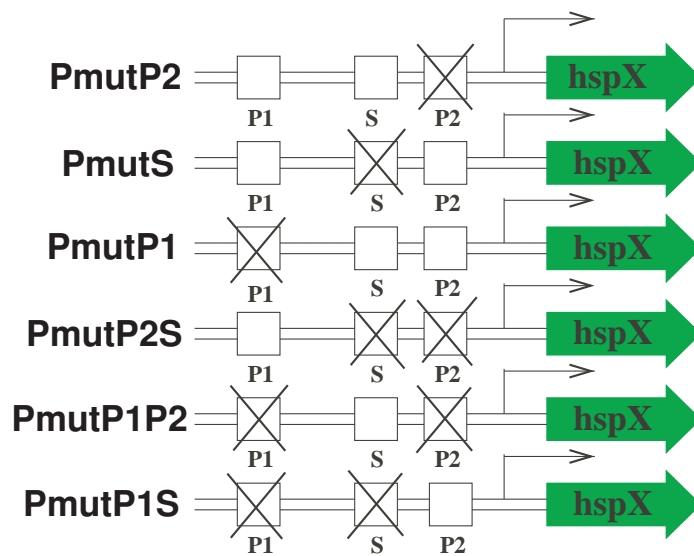


**Fig. 6** Possible mutants by permutation of three binding sites of *hspX* promoter region. The first and the third mutant from top have been studied by Park et al (2003) and behavior of other mutants has been predicted in this study.

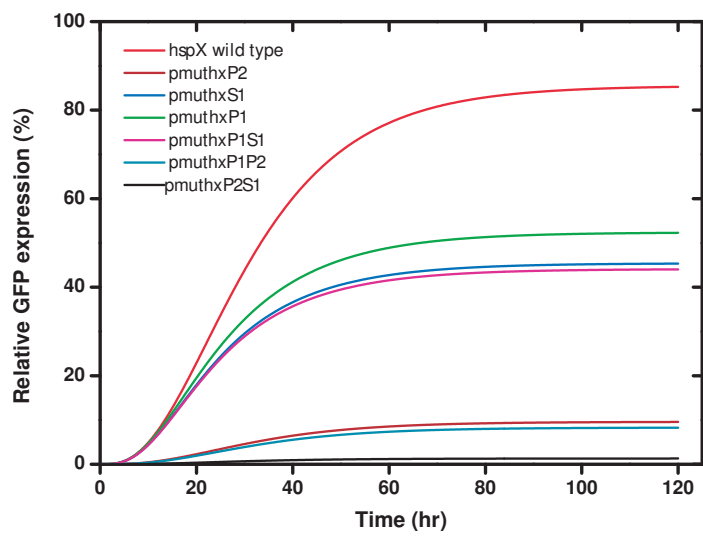


**Fig. 7** Time evolution of wild type *hspX* and all its mutants. All the double mutants except pmuthP2S1 and pmuthP1 have very low expression showing the importance of *P1* binding site.

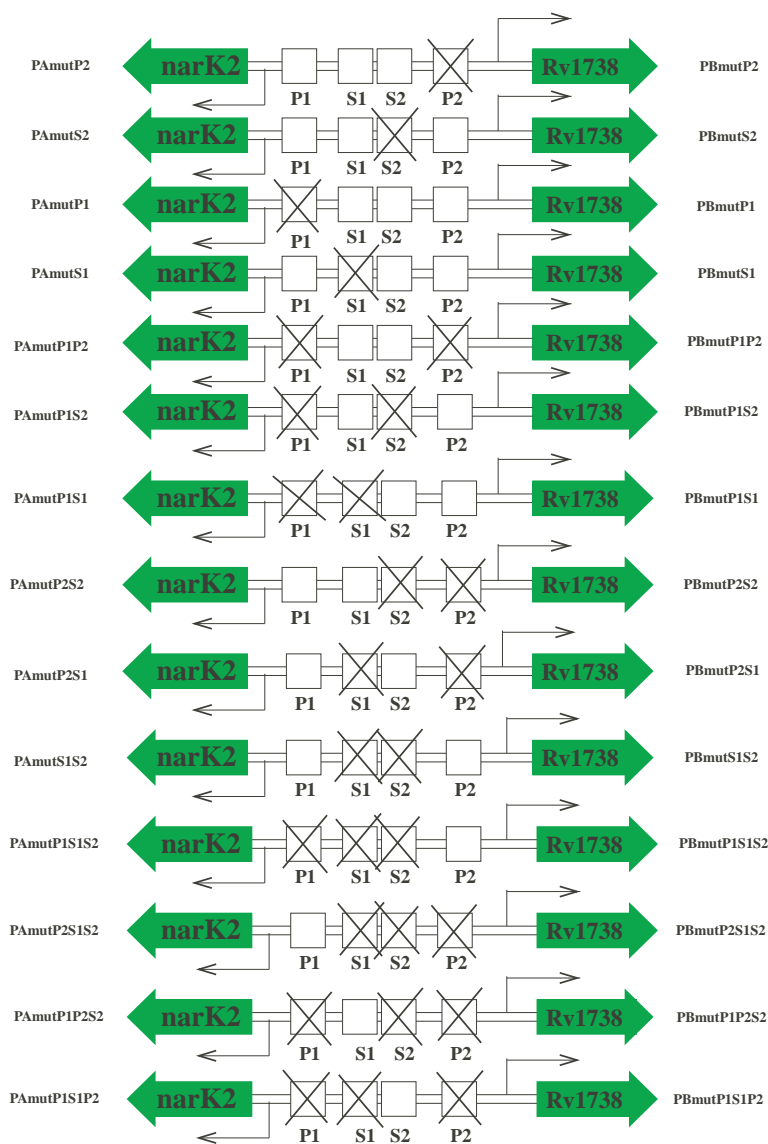


**Fig. 8** Possible mutants by permutation of four binding sites of *narK2*-Rv1738 intergenic promoter region. The first three and the fifth mutant from top have been created by Chauhan and Tyagi (2008b) and behavior of other mutants has been predicted in this study.

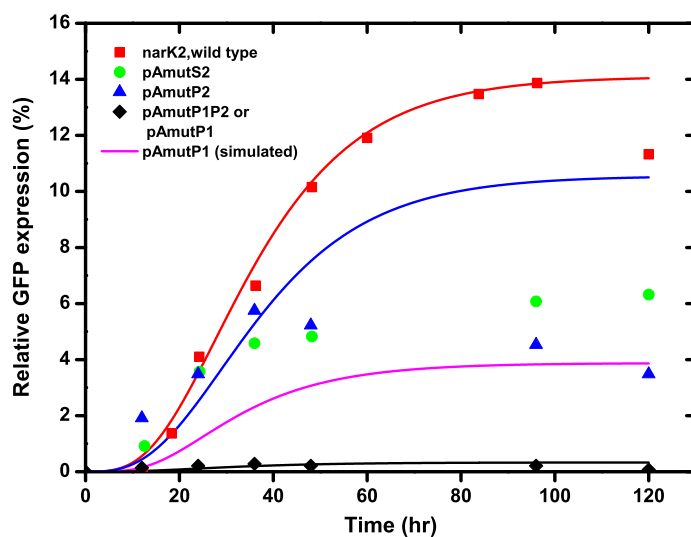


**Fig. 9** Time evolution of relative GFP expression of *narK2* and its mutants. Symbols are taken from Chauhan and Tyagi (2008b) and the continuous lines are results of numerical simulation. According to our model pAmutS2 and pAmutP2 behave equivalently.

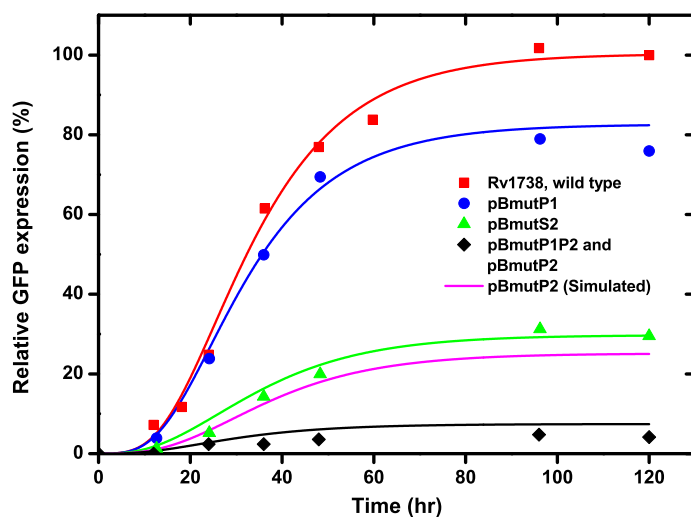


**Fig. 10** Time evolution of relative GFP expression of Rv1738 and its mutants. Symbols are taken from Chauhan and Tyagi (2008b) and the continuous lines are results of numerical simulation.

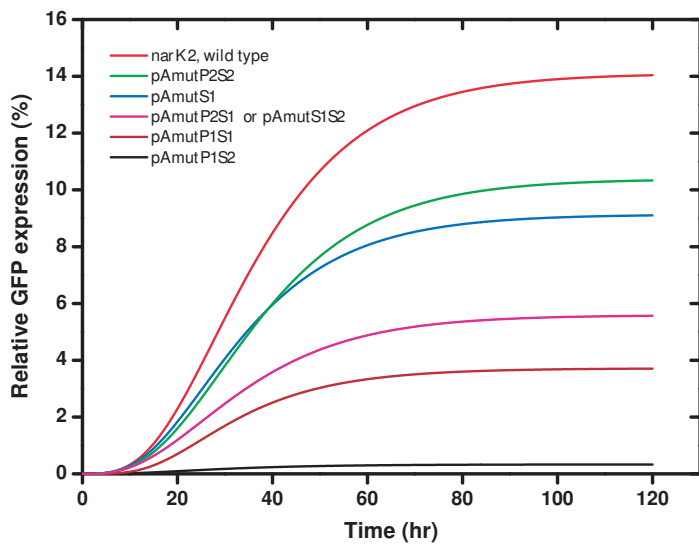


**Fig. 11** Prediction for temporal dynamics of relative GFP expression of *narK2* and its double mutants. According to our model, except pAmutP1S2 others should have detectable expression.

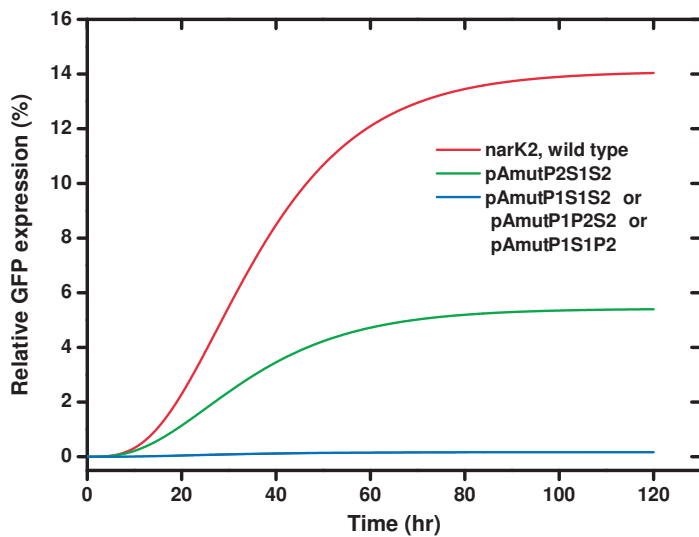


**Fig. 12** Prediction for temporal dynamics of relative GFP expression of *narK2* and its triple mutants in which only pAmutP2S1S2 should have detectable expression.

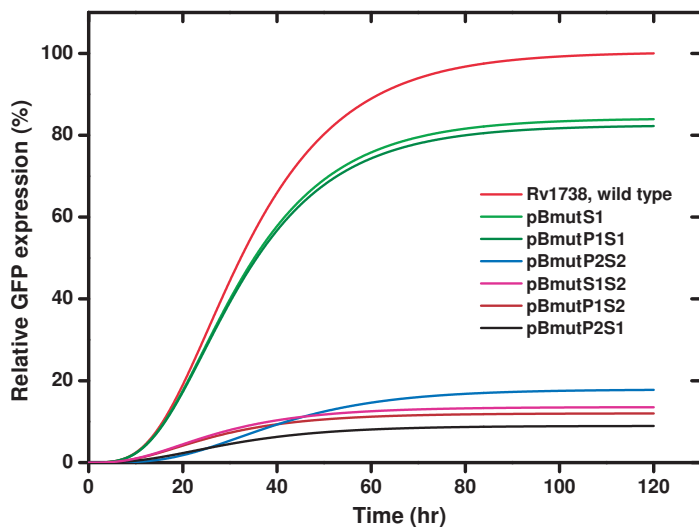


**Fig. 13** Prediction for temporal dynamics of GFP expression of Rv1738 and its double mutants. The expression of the double mutants which have either *P2* or *S2* or both sites mutated are really small. This clarifies the importance of these two sites on the expression of Rv1738 gene.

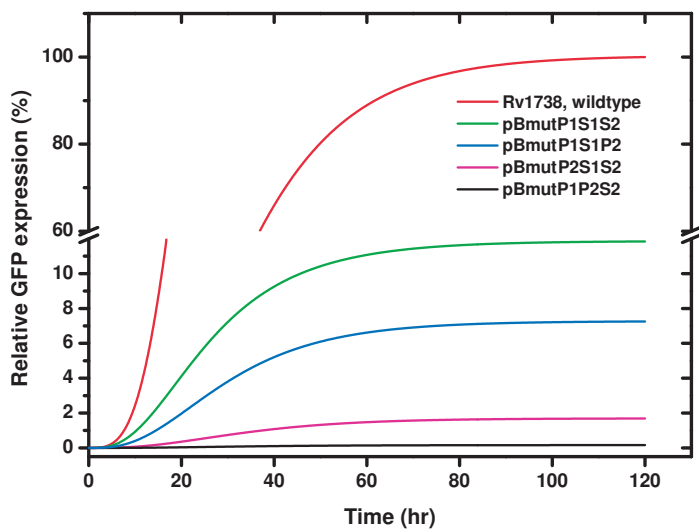


**Fig. 14** Prediction for temporal dynamics of GFP expression of Rv1738 and its triple mutants. All the mutants have very low expression comparative to the wild type strain, which is shown by the axis break.

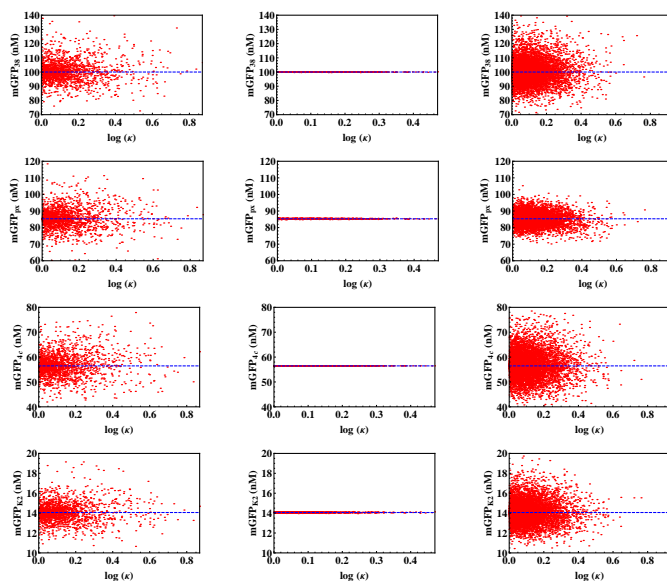


**Fig. 15** Steady state mRNA level as function of total parameter variation  $\log(\kappa)$ . The dashed blue line represents the steady state mRNA level obtained using the unperturbed parameter set. Each red dot represents the same for perturbed parameter set (or subset). 2000 independent simulations have been carried out to create the red dots. In the first column all model parameters have been perturbed. In the second and third column, parameters related to binding-unbinding kinetics and synthesis-degradation kinetics have been modified, respectively.



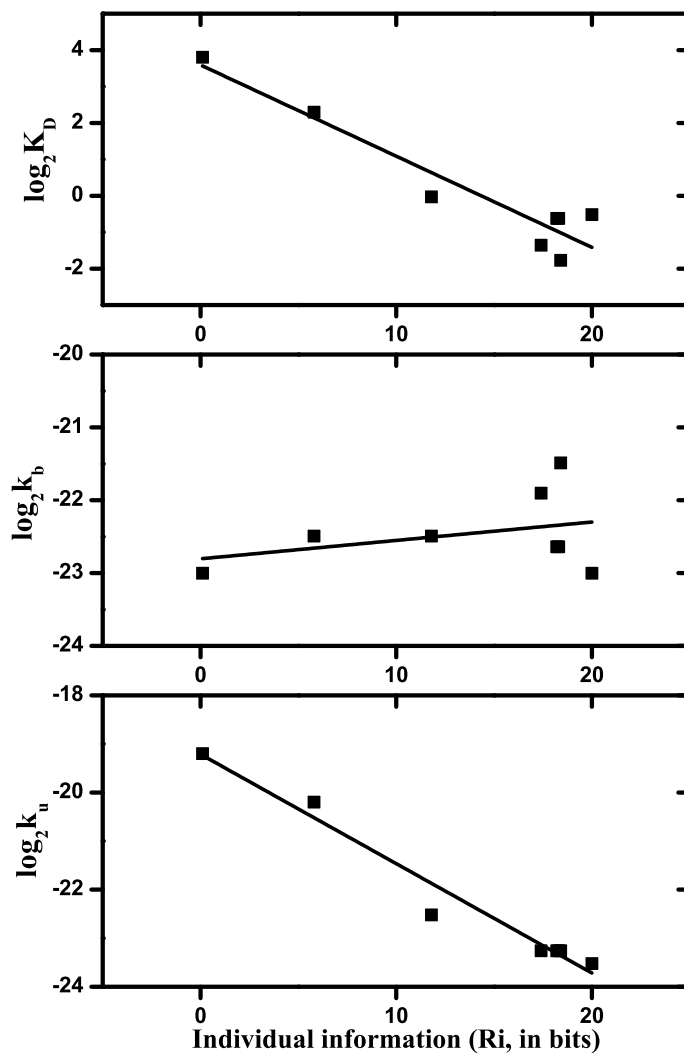


**Fig. 16** Plot of individual information with the logarithmic values of model parameters,  $k_b$ ,  $k_u$  and their ratio  $K_D$ . Solid squares are the logarithm of the parameters and straight lines are the linear fit. This plot shows that logarithmic values of model parameters and the individual information are in a linear relationship.